

Received:

5 May 2017

Revised:

22 August 2017

Accepted:

29 November 2017

Cite as: Gengo Tanaka, Baochun Zhou, Yunfei Zhang, David J. Siveter, Andrew R. Parker. Rods and cones in an enantiornithine bird eye from the Early Cretaceous Jehol Biota.

Heliyon 3 (2017) e00479.

doi: [10.1016/j.heliyon.2017.e00479](https://doi.org/10.1016/j.heliyon.2017.e00479)



CrossMark

# Rods and cones in an enantiornithine bird eye from the Early Cretaceous Jehol Biota

Gengo Tanaka<sup>a</sup>, Baochun Zhou<sup>b,\*</sup>, Yunfei Zhang<sup>b</sup>, David J. Siveter<sup>c</sup>, Andrew R. Parker<sup>d</sup>

<sup>a</sup> *Institute of Liberal Arts and Science, Kanazawa University, Kakuma-machi, Kanazawa 920-1192, Japan*

<sup>b</sup> *Shanghai Natural History Museum, 510 West Beijing Road, Shanghai 200041, China*

<sup>c</sup> *School of Geography, Geology and the Environment, University of Leicester, Leicester LE1 7RH, UK*

<sup>d</sup> *Green Templeton College, University of Oxford, 43 Woodstock Road, Oxford OX2 6HG, UK*

\* Corresponding author.

E-mail address: [zhoubch@sstm.org.cn](mailto:zhoubch@sstm.org.cn) (B. Zhou).

## Abstract

Extant birds have an extensive spectral range of colour vision among vertebrates, but evidence of colour vision among extinct birds has hitherto been lacking. An exceptionally well-preserved extinct enantiornithine fossil bird from the Early Cretaceous Jiufotang Formation (120 Ma) of Liaoning, China, provides the first report of mineralised soft tissue of a bird eye. Cone cells are identified, which have preserved oil droplets falling between wide ranges of size that can be compared with an extant house sparrow. The size distribution of oil droplets of extant birds demonstrates good correlation between size and the detectable wavelength range of the cone cells: UV-sensitive cones contain the smallest oil droplets, while red-sensitive cones possess the largest. The data suggests that this Early Cretaceous bird could have possessed colour vision.

Keywords: Evolution, Palaeobiology, Biological sciences

## 1. Introduction

Having evolved from dinosaurs during the Jurassic, birds then diversified during the Cretaceous (e.g., [Xu et al., 2014](#)). Extant diurnal birds possess colour vision,

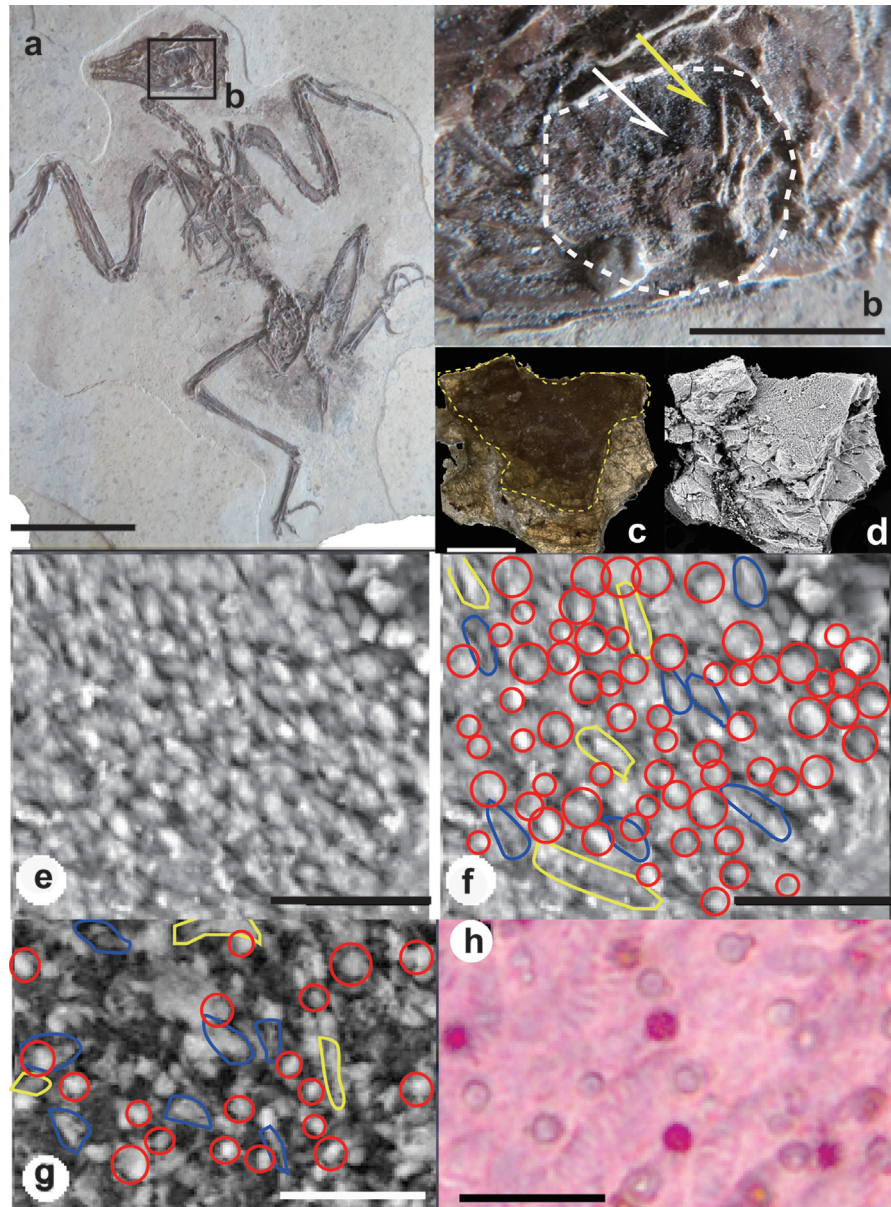


**Fig. 1.** An enantiornithine bird from the Jiufotang Formation, Early Cretaceous, Liaoning, China (a–f) and retina of an extant house sparrow *Passer domesticus* (g,h). (a) Completely preserved specimen (SNHM: 6105). (b) Enlarged eye region of (a) showing eye orbit within the white dotted line, black material (white arrow) and sample point (yellow arrow) of the fragment of (c). (c) Digital microphotograph of an eye fragment. (d) SEM image of an eye fragment. (e) SEM of cone and rod cells with their oil droplets. (f) Labelled image of (e) showing position of oil droplets (red circles), cone (blue solid line) and rod (yellow solid line) cells. (g) SEM image of rods (yellow solid line), cones (blue solid line) and oil droplets (red circles). (h) Transmitted microphotograph of oil droplets. Scale bars: a = 2 cm; b = 5 mm; c,d = 100  $\mu\text{m}$ ; e–h = 10  $\mu\text{m}$ .

**Table 1.** Area of oil droplets in an extant house sparrow *Passer domesticus*. The cone type to which each oil droplet belongs was determined based on the methods of Kolb and Jones (1982).

No.	Cone type	Area of oil droplet ( $\mu\text{m}^2$ )	No.	Cone type	Area of oil droplet ( $\mu\text{m}^2$ )
1	green	2.9	159	red	2.7
2	green	2.8	160	double	2.6
3	blue	1.1	161	blue	1.8
4	double	2.8	162	double	2.7
5	red	3.8	163	violet	0.6
6	red	3.0	164	double	2.7
7	blue	0.9	165	red	3.6
8	red	3.0	166	blue	0.9
9	green	2.0	167	green	2.8
10	red	3.8	168	red	3.4
11	red	3.6	169	green	2.1
12	blue	1.4	170	violet	0.6
13	green	2.7	171	violet	0.7
14	red	3.2	172	red	4.3
15	red	4.2	173	double	3.1
16	double	3.8	174	double	3.0
17	green	2.3	175	double	2.7
18	double	2.5	176	blue	1.0
19	green	3.1	177	double	2.9
20	green	3.1	178	green	2.3
21	green	2.0	179	violet	0.4
22	green	2.3	180	violet	0.7
23	green	2.7	181	green	3.3
24	green	2.5	182	green	3.0
25	green	2.3	183	violet	0.7
26	green	2.3	184	red	3.9
27	green	2.5	185	violet	0.4
28	green	3.2	186	green	3.2
29	red	3.1	187	double	2.2
30	green	2.4	188	double	3.0
31	green	2.5	189	violet	0.9
32	green	3.0	190	green	2.8
33	green	2.1	191	red	4.1
34	double	2.5	192	double	3.3
35	green	2.2	193	double	3.2

(Continued)

**Table 1.** (Continued)

No.	Cone type	Area of oil droplet ( $\mu\text{m}^2$ )	No.	Cone type	Area of oil droplet ( $\mu\text{m}^2$ )
36	violet	0.6	194	double	2.9
37	double	2.2	195	red	3.9
38	green	1.7	196	green	3.2
39	double	2.3	197	double	2.7
40	blue	1.0	198	blue	0.9
41	green	1.9	199	green	3.4
42	double	3.2	200	violet	0.8
43	double	3.4	201	violet	0.9
44	double	2.5	202	violet	0.7
45	double	2.7	203	violet	0.4
46	double	3.4	204	blue	1.2
47	green	3.4	205	red	3.5
48	double	2.9	206	violet	1.0
49	double	3.0	207	double	3.0
50	red	4.2	208	red	3.5
51	double	2.3	209	double	3.1
52	double	2.6	210	green	3.1
53	green	2.9	211	double	2.6
54	double	3.0	212	green	2.5
55	red	4.1	213	blue	0.6
56	red	4.5	214	violet	0.6
57	double	3.0	215	violet	0.5
58	double	3.2	216	violet	0.7
59	double	2.9	217	violet	0.7
60	double	2.9	218	blue	1.1
61	green	2.4	219	violet	0.7
62	red	4.0	220	red	3.9
63	violet	1.1	221	double	2.8
64	double	2.8	222	double	2.8
65	double	3.2	223	double	2.5
66	double	2.5	224	double	3.3
67	violet	0.7	225	blue	0.7
68	violet	0.9	226	double	3.4
69	double	2.2	227	red	3.9
70	red	3.2	228	double	2.6
71	double	2.5	229	red	3.8
72	double	2.1	230	green	3.3
73	red	2.8	231	double	2.8

(Continued)

**Table 1.** (Continued)

No.	Cone type	Area of oil droplet ( $\mu\text{m}^2$ )	No.	Cone type	Area of oil droplet ( $\mu\text{m}^2$ )
74	blue	1.6	232	blue	1.4
75	double	2.4	233	red	3.2
76	double	3.2	234	blue	1.0
77	red	3.4	235	green	2.9
78	blue	1.1	236	violet	0.9
79	blue	1.6	237	double	2.3
80	red	3.5	238	violet	0.5
81	double	3.2	239	double	2.7
82	green	3.5	240	double	2.5
83	red	3.4	241	green	2.6
84	double	2.3	242	double	1.9
85	blue	1.4	243	double	2.5
86	blue	1.2	244	double	2.5
87	double	2.8	245	blue	0.4
88	violet	1.0	246	blue	0.8
89	red	2.9	247	double	2.3
90	green	1.5	248	double	2.6
91	green	2.1	249	violet	0.3
92	violet	1.2	250	violet	0.6
93	double	3.3	251	double	2.5
94	double	3.7	252	red	3.5
95	double	2.4	253	double	2.1
96	red	3.4	254	red	3.4
97	double	3.2	255	double	2.7
98	green	2.7	256	violet	0.6
99	red	3.4	257	double	3.2
100	double	2.5	258	violet	0.5
101	blue	1.3	259	double	3.1
102	green	2.8	260	double	2.7
103	blue	1.0	261	violet	0.5
104	red	3.6	262	green	2.8
105	double	2.6	263	violet	0.9
106	violet	1.1	264	double	2.3
107	double	2.9	265	red	4.0
108	blue	0.7	266	violet	0.8
109	red	4.3	267	violet	0.9
110	green	2.7	268	green	2.7
111	green	2.9	269	violet	1.1

(Continued)

**Table 1.** (Continued)

No.	Cone type	Area of oil droplet ( $\mu\text{m}^2$ )	No.	Cone type	Area of oil droplet ( $\mu\text{m}^2$ )
112	green	2.7	270	violet	1.0
113	green	2.5	271	green	2.8
114	green	2.0	272	violet	0.8
115	blue	0.9	273	double	3.0
116	green	3.8	274	blue	0.9
117	blue	1.7	275	double	3.2
118	violet	1.1	276	green	2.6
119	violet	1.3	277	violet	0.7
120	violet	1.3	278	violet	0.7
121	violet	1.0	279	double	3.5
122	red	2.9	280	double	3.6
123	double	2.0	281	red	3.9
124	blue	1.3	282	double	2.5
125	violet	1.1	283	green	2.7
126	violet	0.9	284	blue	0.8
127	double	2.5	285	green	3.1
128	red	3.3	286	blue	0.9
129	blue	1.4	287	violet	0.5
130	violet	1.0	288	green	2.6
131	violet	0.8	289	green	3.6
132	green	2.5	290	green	3.5
133	violet	1.0	291	double	2.5
134	red	2.8	292	red	3.9
135	violet	0.5	293	red	3.8
136	double	2.3	294	double	3.0
137	green	2.9	295	green	3.3
138	double	1.9	296	violet	1.2
139	red	3.2	297	green	3.2
140	double	2.6	298	red	3.8
141	double	2.4	299	violet	0.7
142	double	2.7	300	violet	0.7
143	green	2.3	301	double	3.1
144	red	2.5	302	red	3.6
145	double	2.2	303	green	2.5
146	violet	0.9	304	double	3.4
147	red	4.1	305	double	3.0
148	double	3.0	306	double	3.1
149	green	2.4	307	red	3.1

(Continued)

**Table 1.** (Continued)

No.	Cone type	Area of oil droplet ( $\mu\text{m}^2$ )	No.	Cone type	Area of oil droplet ( $\mu\text{m}^2$ )
150	red	2.8	308	double	2.7
151	double	3.0	309	double	2.3
152	double	3.0	310	green	2.3
153	green	2.4	311	red	3.3
154	double	3.2	312	double	2.7
155	red	3.0	313	green	2.1
156	red	2.5	314	red	4.0
157	blue	1.2	315	double	3.5
158	double	2.5	316	blue	1.2

involving five types of cone cells that together can discriminate a spectrum from ultraviolet to red (Hart, 2001a; Hart, 2004; Cuthill, 2006; Bowmaker, 2008). The discovery of fossilised melanosomes in some Mesozoic animals suggests that they were adapted to a colourful world in the geological past (Li et al., 2010; Li et al., 2012; Zhang et al., 2010; Barden et al., 2011). However, compelling evidence of colour vision in fossil birds has not been reported because photoreceptors are not usually fossilised. A fossilised visual photoreceptor (Fröhlich et al., 1992; Duncan and Briggs, 1996; Tanaka et al., 2009; Tanaka et al., 2014; Schoenemann and Clarkson, 2013; Vannier et al., 2016) or a mold equivalent (Schoenemann et al., 2012) has only been reported in a total of six fossil taxa: five arthropods and one fish. Thus, examples of fossilised visual photoreceptors from extinct birds would shed light on the retinal anatomy of fossil birds and allow an assessment of whether these taxa also had the ability to distinguish colours. The spectral sensitivity of a cone retinal photoreceptor depends upon its particular combination of an opsin photopigment and a coloured oil droplet, which is located in the distal tip of the inner segment of the cone cell and functions as a cut-off filter for incoming light (Hart, 2001a; Hart, 2004; Bowmaker, 2008; Ohtsuka, 1985; Kram et al., 2010). The filtering of the specific wavelength range is also achieved by the ellipsoid positioned in front of the oil droplet (Wilby et al., 2015). These are found in some fish (e.g. sturgeon and lungfish), amphibians, reptiles, and birds (Bowmaker, 2008; Cheung et al., 2013). The colour of the oil droplets represents the wavelengths of light that are transmitted; e. g., red oil droplets transmit long wavelength (“red”) light, whereas colourless (to the human eye) oil droplets absorb the shortest (UV-A) wavelength light for vision in many animals (Kolb and Jones, 1982). Furthermore, the size of the oil droplet is correlated to its colour: for example, in the dorsal area of turtle retinas, red oil droplets are largest (diameter = 8.5  $\mu\text{m}$ ), yellow oil droplets are mid-sized (7.3–7.0  $\mu\text{m}$ ), and colourless oil droplets are the smallest (5.2–5.6  $\mu\text{m}$ ) (Ohtsuka, 1989). In the mid-peripheral area of the retina of chicken, the size of red oil droplets ranges between

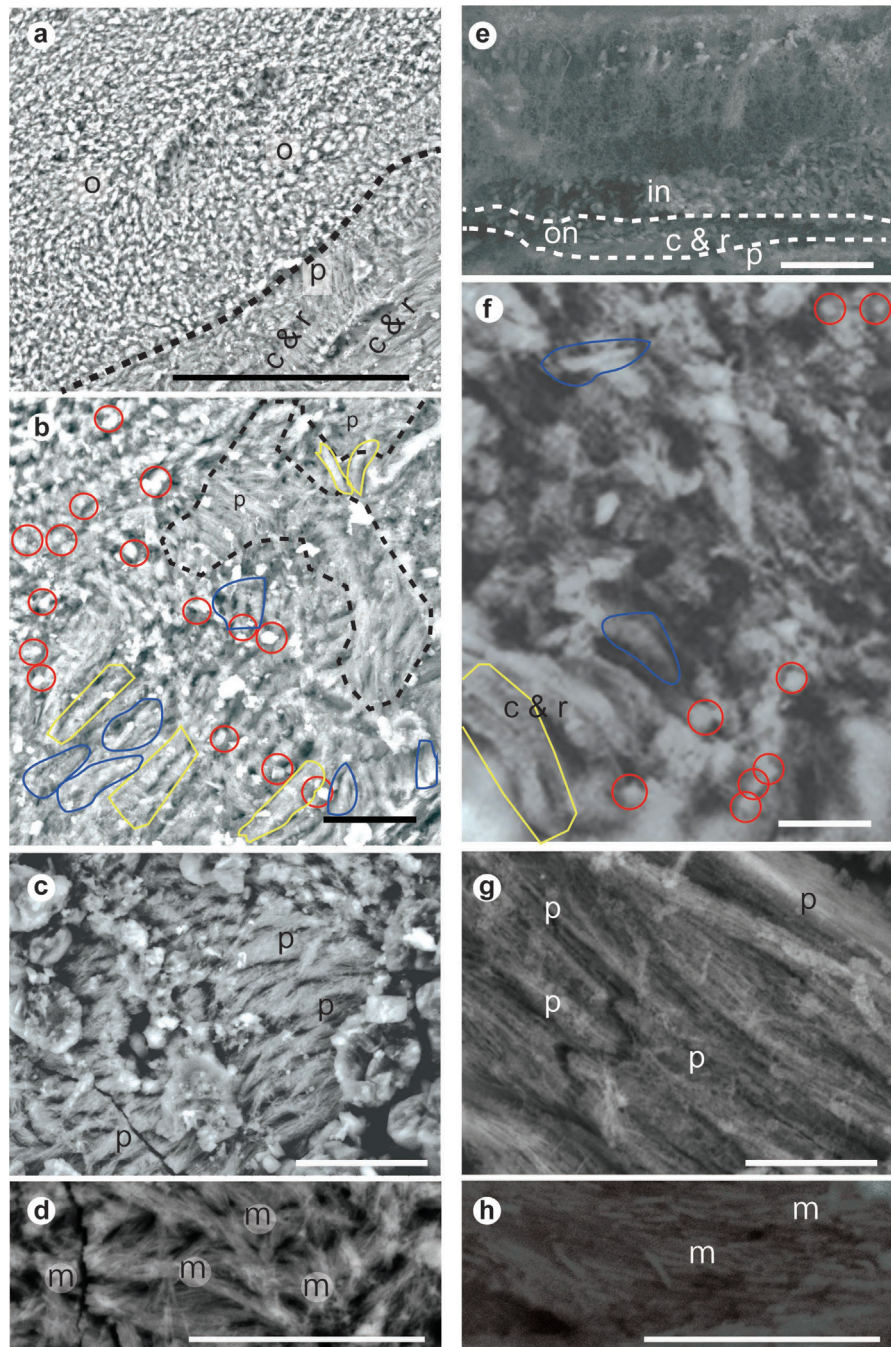


**Fig. 2.** SEM images of the retinas of an Early Cretaceous enantiornithine bird and an extant house sparrow *Passer domesticus*. (a) A fragment of the retina of the fossil bird preserving many oil droplets (o) in the upper left region of the broken line, pigment epithelium (p), and rods (r) and cones (c). (b) Magnified image of (a) showing oil droplets (red circles) and pigment epithelium (p), and rods (yellow solid line) and cones (blue solid line). (c) A fragment of the fossil pigment epithelium (p) with preserved fine fibrous structures. (d) An enlargement of the fossil pigment epithelium containing elongate melanosomes (m). (e) Transverse section of the retina of an extant house sparrow. The retina is composed of pigment epithelium (p), cones (c) and rods (r) with oil droplets, an outer nuclear layer (on), and an inner nuclear layer (in) oriented in the proximal-distal plane of the eyeball. (f) A fragment of the retina of an extant house sparrow. Many oil

droplets (red circles) were removed from cones. (g) Pigment epithelium (p) of an extant house sparrow. (h) An enlargement of pigment epithelium of an extant house sparrow containing elongate melanosomes (m). Scale bars: a, e = 50  $\mu\text{m}$ ; b–d, f–h = 10  $\mu\text{m}$ .

7.9 and 6.1  $\mu\text{m}$ , yellow oil droplets between 6.4 and 3.6  $\mu\text{m}$ , and colourless oil droplets between 3.5 and 2.8  $\mu\text{m}$  (Kram et al., 2010).

The lower Cretaceous (120 Ma) Jehol Konservat-Lagerstätte in western Liaoning, China, yields exquisitely preserved organisms from disparate taxa including

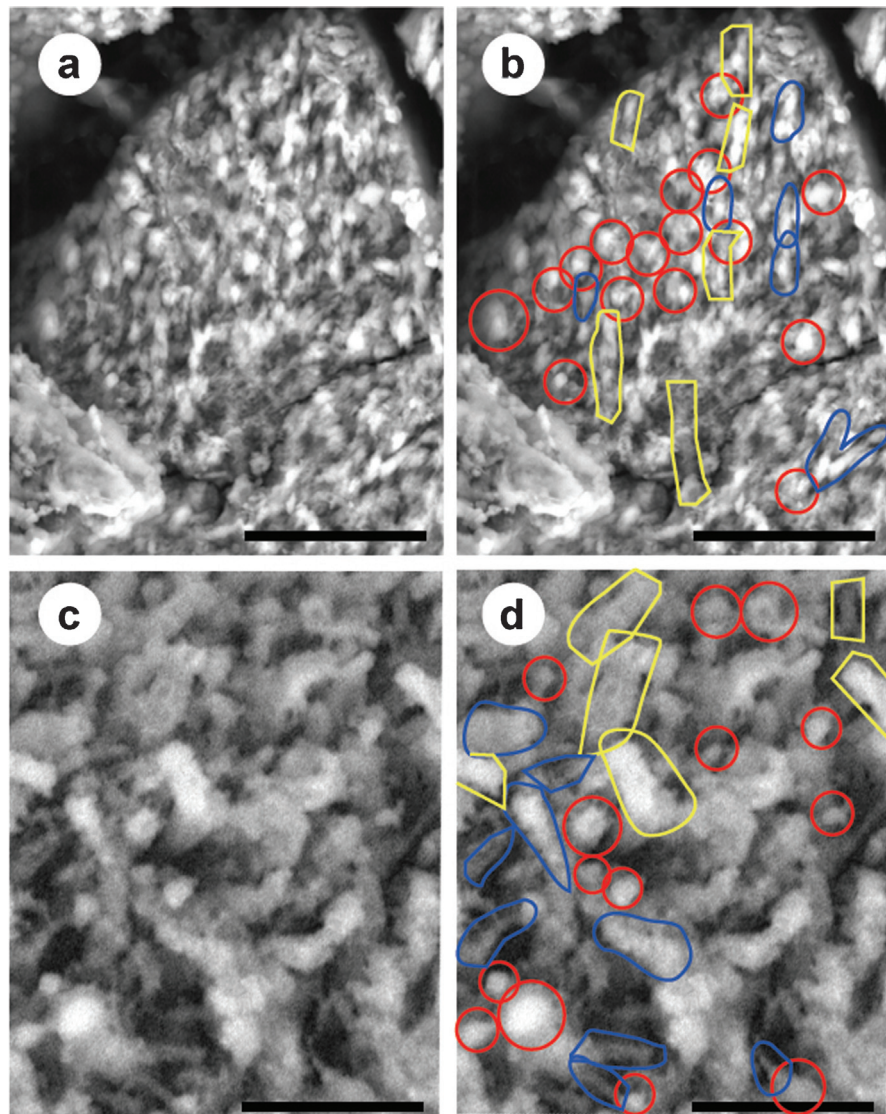


**Fig. 3.** Unlabelled (a, c) and labelled (b, d) SEM images of an Early Cretaceous enantiornithine bird and an extant house sparrow *Passer domesticus*. (a, b) A fragment of the retina of the fossil bird. (c, d) A freeze dried fragment of the retina of the house sparrow. Labelled images indicate rods (yellow solid line), cones (blue solid line) and oil droplets (red circles). Scale bar = 10  $\mu\text{m}$ .

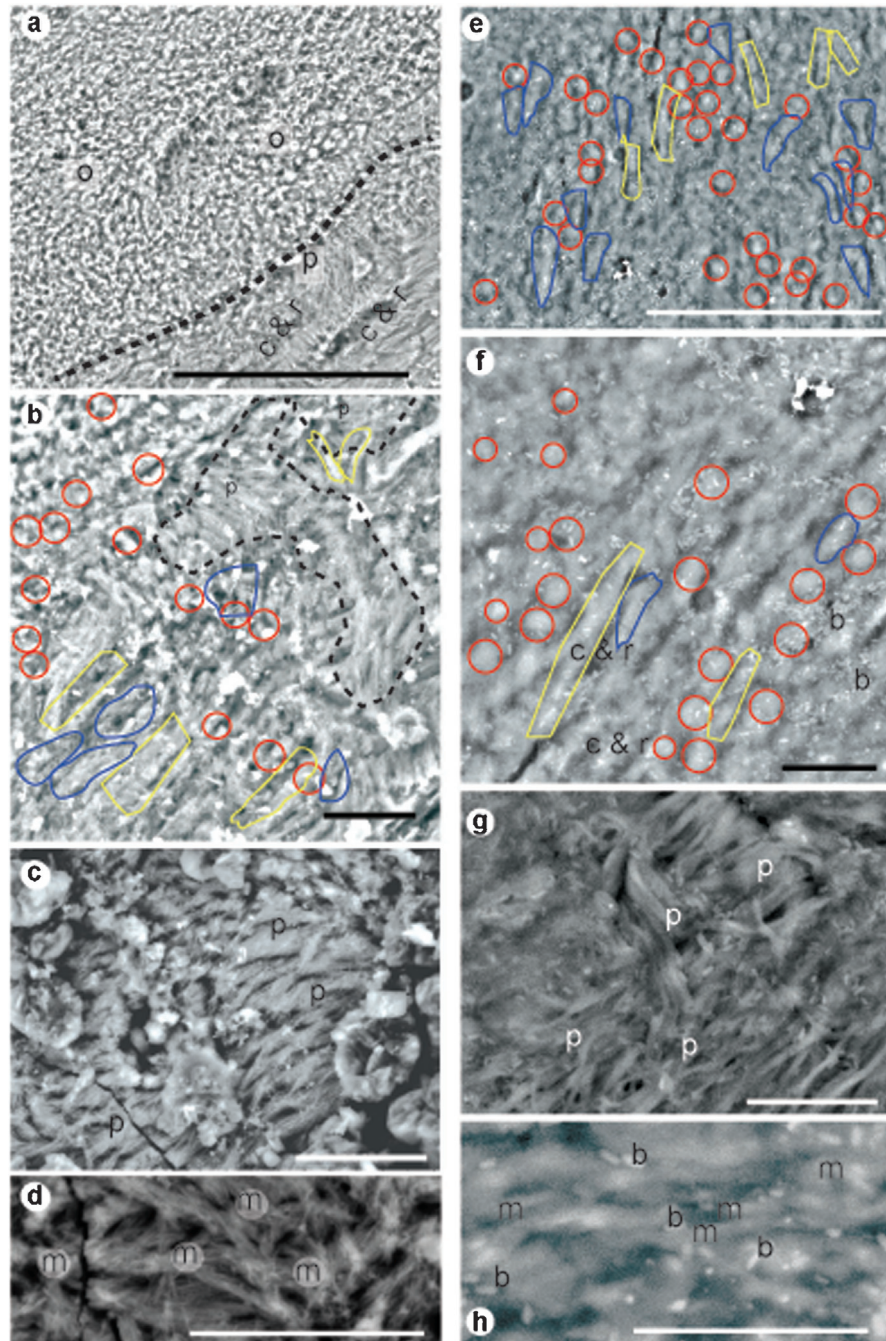


**Fig. 4.** SEM images of the retinas of an Early Cretaceous enantiornithine bird and a natural dried extant house sparrow *Passer domesticus*. (a) A fragment of the retina of the fossil bird preserving many oil droplets (o) in the upper left region, pigment epithelium (p), and rods (c) and cones (c). (b) Enlarged image of (a) showing oil droplets (red circles), pigment epithelium (p), and rods (yellow solid line) and cones (blue solid line). (c) A fragment of the fossil pigment epithelium (p) with preserved fine fibrous structures. (d) An enlargement of the fossil pigment epithelium containing elongate melanosomes (m). (e) The photosensitive organ of an extant house sparrow that is composed of cones (blue solid line) and rods (yellow solid line) with oil droplets (red circles). (f) An enlargement of (e). Oil droplets (red circles) and cone and rods (c & r) are rather flattened but associated with each other. (g) Pigment

epithelium (p) of an extant house sparrow. (h) An enlargement of pigment epithelium (p) of an extant house sparrow containing elongate melanosomes. Melanosomes (m) are distinguished from bacteria (b) by their longer shape. Scale bars: a, e = 50  $\mu\text{m}$ ; b–d, f–h = 10  $\mu\text{m}$ .

feathered dinosaurs, early birds, mammals with hair, complete arthropods, and plants (Zhou et al., 2003). Fine details are preserved because the organic material was originally transported by a pyroclastic density current and sealed within the pyroclastic flow (Jiang et al., 2014). The subadult fossil bird specimen reported herein belongs to a species of Enantiornithes documented from the Early Cretaceous of Liaoning (Chiappe and Walker, 2002).

## 2. Material and methods

The fossil bird specimen studied herein (Fig. 1a) is a subadult stage of an unnamed enantiornithine species (personal communication with Prof. Zhonghe Zhou, Institute of Vertebrate Paleontology and Paleoanthropology, Chinese Academy of Science). A small fragment of retina measuring approximately 4 mm<sup>2</sup> was removed from the posterodorsal margin of the fossil bird eye using a craft knife (Fig. 1b–d). It was placed on a stub, viewed under a binocular optical microscope (Olympus SZH10), uncoated, and observed in a SEM (Hitachi TM-1000) under a low vacuum at the Aitsu Marine Station of Kumamoto University, Japan. The section of fossilised retinal material was observed using a confocal laser microscope (VK-9500, KEYENCE) at the Kumamoto Industrial Research Institute. An extant house sparrow, *Passer domesticus* (eye diameter 0.7 cm, body length 10 cm) and a Japanese quail, *Coturnix japonica* (eye diameter 1.1 cm, body length 15 cm), were selected for comparative purposes because they have a body length and/or eyeball size similar to the fossil bird (eye diameter 0.65 cm). Furthermore, *P. domesticus* and *C. japonica* are distantly related (Dobson, 2012), which is preferable for the purpose of excluding phylogenetic constraint.

The freshly-killed *P. domesticus* and *C. japonica* were obtained from the company Moukinya. The eyeballs of both birds were removed using a craft knife and fixed in phosphate buffered saline solution (PBS). Each retina was removed from the eyeball in the PBS and was rinsed with fresh PBS. Each retina of the two extant birds was partially freeze-dried for SEM observations.

In order to check for morphological alternations of retinal tissues, another naturally dried house sparrow eye was investigated to provide a control for early diagenesis.

To determine the precise size-colour relationship of the oil droplets of the extant quail and house sparrow, each retinal sheet was removed from the pigment epithelium in PBS by levering with a needle. The retinal fragment was then mounted on a slide glass and covered with a cover slip. The size of the same coloured oil droplets varies between different regions of the same eye (Hart, 2004),

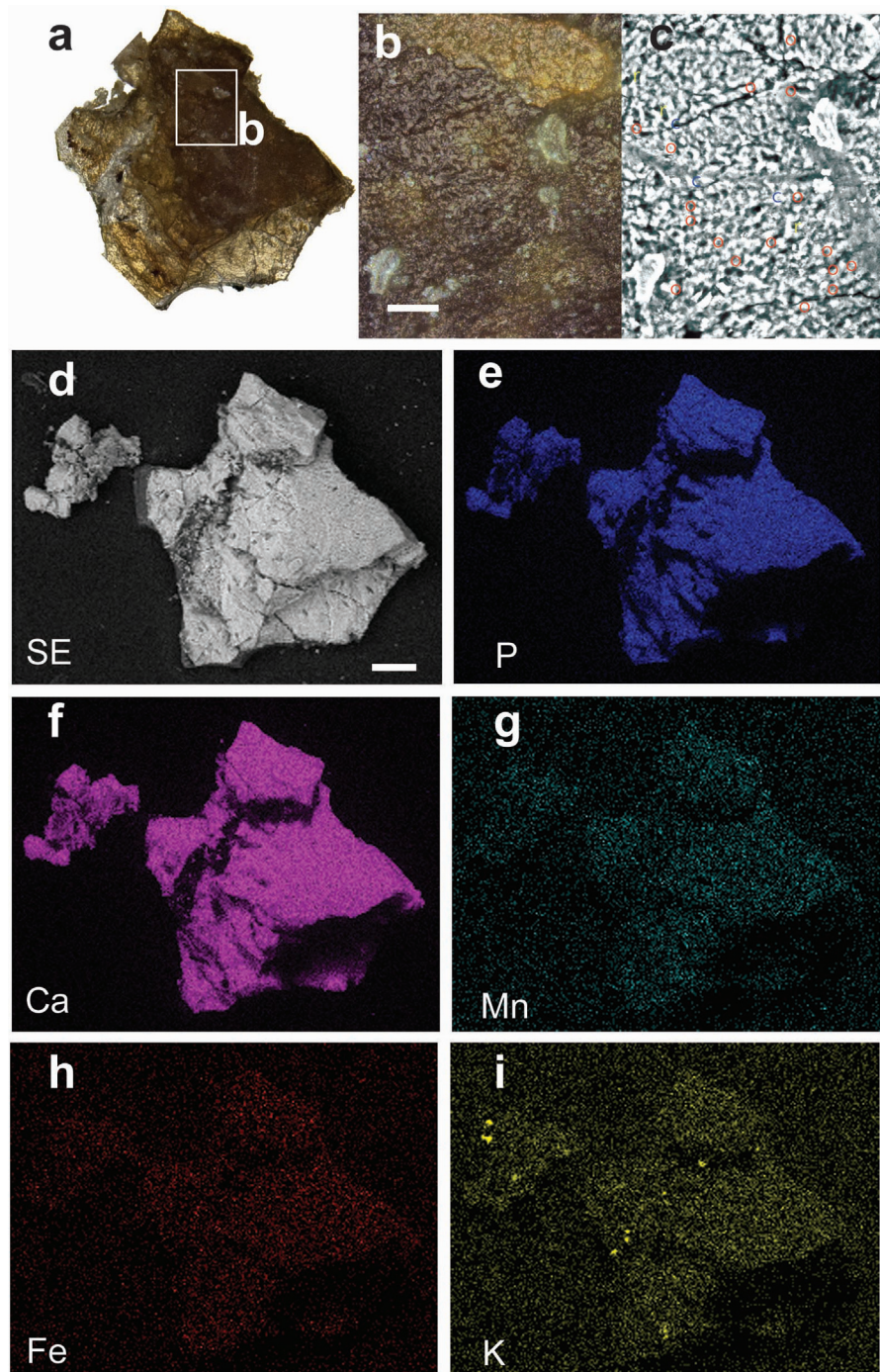


**Fig. 5.** A fragment of fossil retina of an Early Cretaceous enantiornithine bird and the distribution of elements within. (a) Digital microphotographs of a retinal region. (b,c) Enlargement of an area observed by laser microscope (b) and SEM (c). (d) Backscattered electron image of (a). (e–i) Distribution of the elements P, Ca, Mn, Fe, and K.

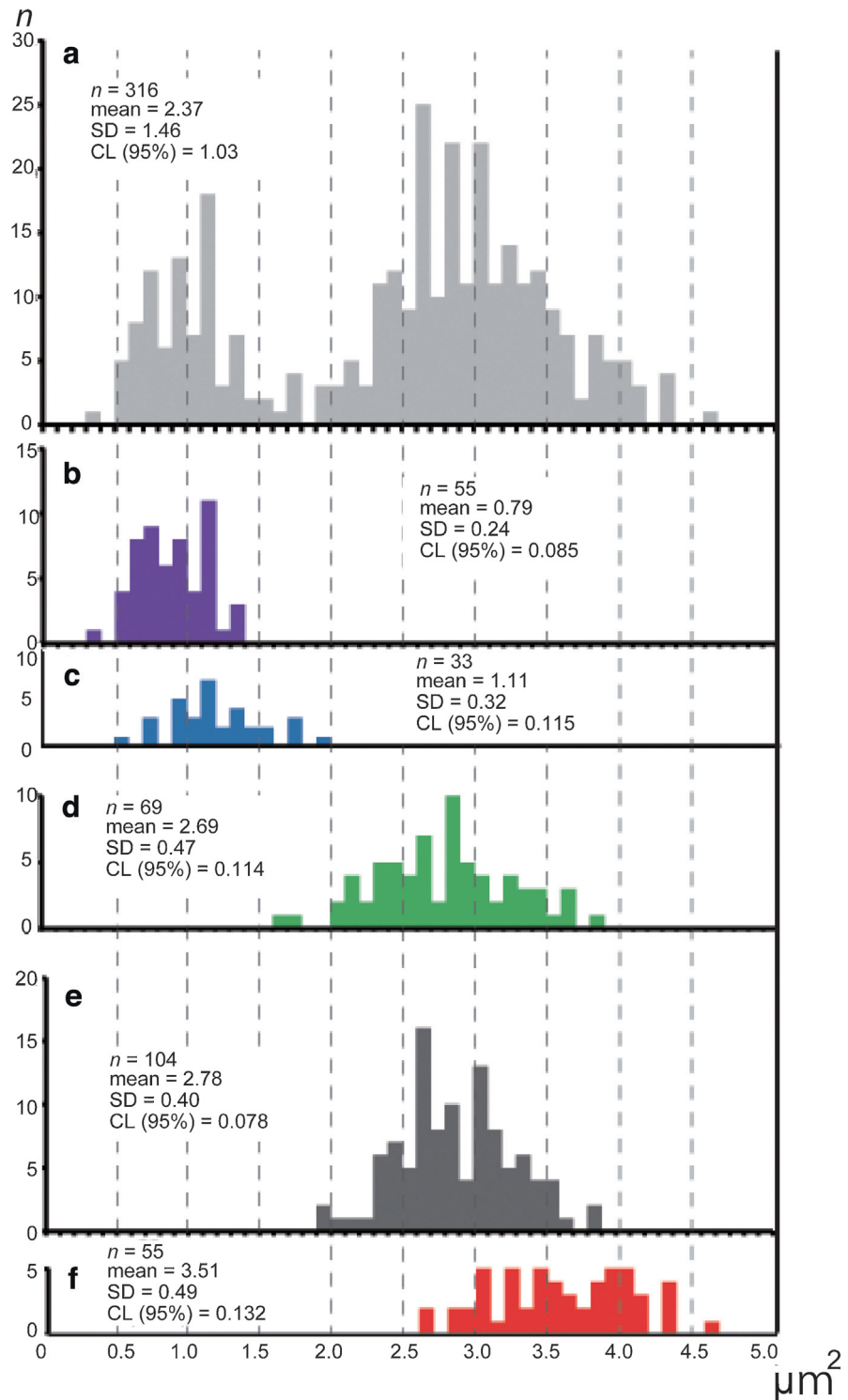


**Fig. 6.** Frequency distribution of area of oil droplets of an extant house sparrow *Passer domesticus*. (a) Histogram of all oil droplet sizes. (b–f) Histogram of sizes for each type of coloured oil droplet: clear (b), light blue (c), yellow (d), dark green (e), and red (f) (these are correlated with ultraviolet sensitive single cones [UVS], short-wavelength sensitive single cones [SWS], medium-wavelength sensitive

single cones [MWS], intermediate sensitive double cones [IWS], and long-wavelength sensitive single cones [LWS], respectively). SD = Standard deviation, CI = Confidence interval.

so only the retinal sheet removed from the marginal area of the eyeball (similar to that studied in the fossil eye) was used in this study.

The oil droplets were observed under a transmitted light microscope (Olympus CH40) with a digital video camera (Nikon DS-Vi1), and images were captured using 'Nis-Element v. 4.0' software. The images were saved as TIFF files using graphic software (Adobe Photoshop, version 7.01). The area of each oil droplet was calculated using area-calculating software in Image J (Rasband, 1977–2012). The colour of the oil droplet was identified by eye under a transmitted light microscope. The cone type, such as ultraviolet sensitive (UVS), short-wavelength sensitive (SWS), medium-wavelength sensitive (MWS), and long-wavelength sensitive (LWS) was determined based on Table 1 of Hart (2001b). The area data was initially preserved as an .xls file. By using free statistical software (Takeyasu, 2011), a Mann-Whitney *U* test (Faul et al., 2007) was performed to determine whether the values of the areas between different coloured oil droplets in the extant house sparrow were statistically distinguishable. Statistical Power ( $1-\beta$ ) was calculated with G\*Power software (ver 3.1.9.2) for checking the type II error (Faul et al., 2007). By using the R packages version 3.1.3 (R Development Core Team, 2013), Akaike information criterion (AIC) analysis (Akaike, 1974) was conducted to examine the relative quality of statistical models for a given set of data.

Elemental distribution and spectral patterns were obtained using energy-dispersive X-ray fluorescence (EDXRF) microscopy (XGT-5000 V, HORIBA) at 20 kV accelerated voltage and 5.2 mA probe current, using mono-capillary primary optics to focus the X-ray beam to a diameter of 10  $\mu\text{m}$ . A fragment of fossil retina was attached to an aluminum stage; its position in the vacuum chamber was adjusted using a motorized xyz platform and viewed using three integrated colour video cameras. An area of 256  $\mu\text{m} \times 200 \mu\text{m}$  was analysed under full vacuum using 50 mm steps and 200,000 frames to provide two-dimensional distribution maps and spectral patterns of three points for seven elements, Mg, Si, P, K, Ca, Mn and Fe. The EDXRF analyses were performed at the Centre of Advanced Instrumental Analysis, Kyushu University.

All illustrated specimens are deposited in Shanghai Natural History Museum, Branch of Shanghai Science and Technology Museum.

### 3. Results

The eye of the fossil enantiornithine specimen contains black material, like that of a fossil fish (Tanaka et al., 2014), and fills the eye orbit (Fig. 1a,b). Digital microphotographs and scanning electron micrographs (SEMs) of the black material

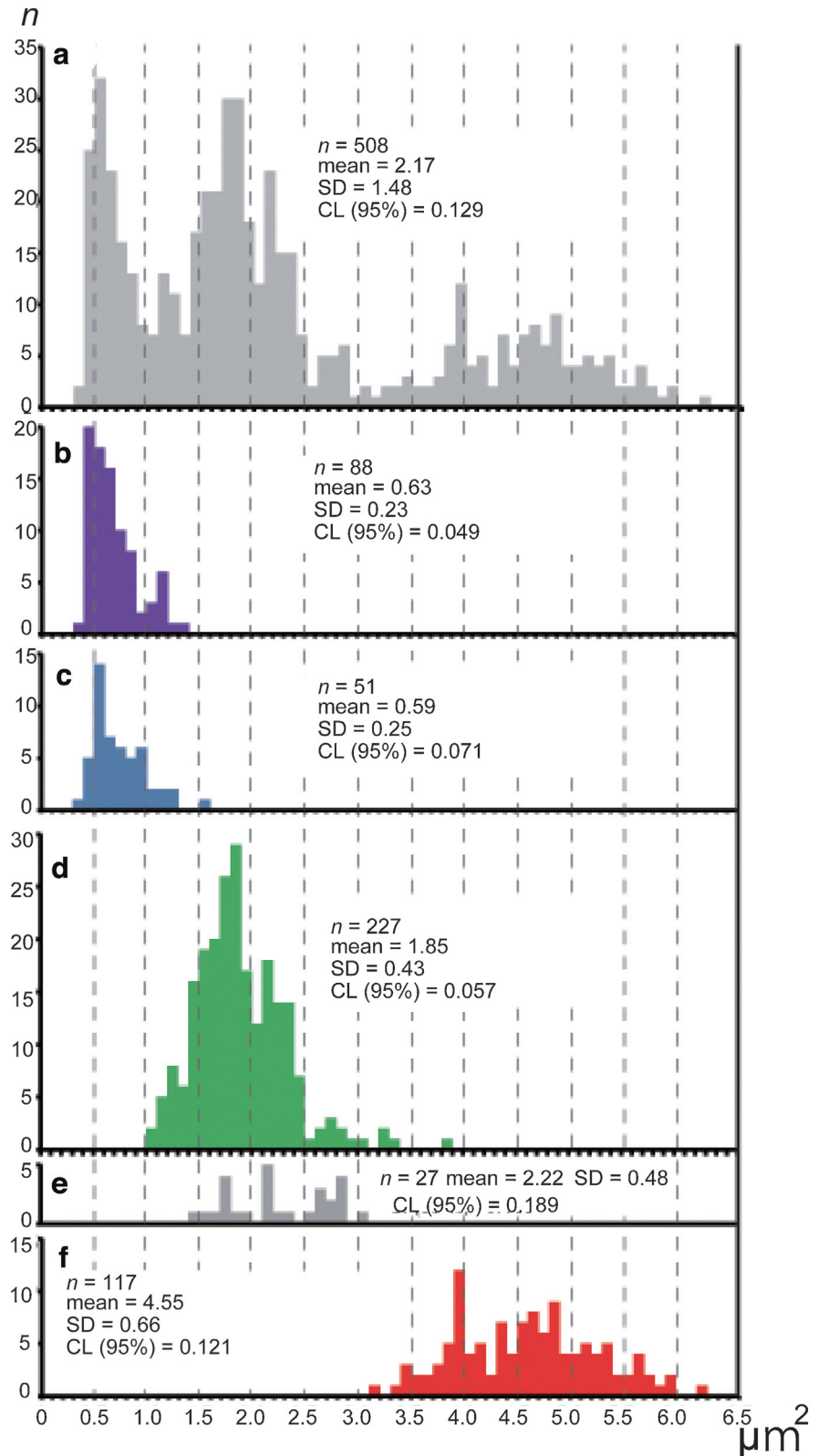


**Fig. 7.** Frequency distribution of area of oil droplets of an extant Japanese quail *Coturnix japonica*. (a) Histogram of all oil droplet size. (b–f) Histogram of sizes for each type of coloured oil droplet: clear (b), light blue (c), yellow (d), dark green (e), and red (f) (these are correlated with ultraviolet sensitive single cones [UVS], short-wavelength sensitive single cones [SWS], medium-wavelength sensitive single cones [MWS], unknown sensitive single cones [UWS], intermediate sensitive double cones [IWS], and long-wavelength sensitive single cones [LWS], respectively). SD = Standard deviation, CI = Confidence interval.

and adjacent bone reveal morphological differences: the coarse surface of the black material (the area surrounded by a yellow dotted line in Fig. 1c) is clearly distinguished from that of the bone, which has a smooth surface with several Haversian canals (Fig. 1c,d). The black material contains three-dimensional, mineralized outer cones and oil droplets (Figs. 1e,f; 2a,b and 3a,b). The shape of the cones and droplets is the same as those of the extant house sparrow (Figs. 1e–h; 2a,b,e,f; 3 and 4), although the oil droplets in the fossilised material (Figs. 1e,f; 2a,b; 3 and 5b) lack colour. The diameter of the oil droplets in both the fossil bird and the extant house sparrow ranges from 2  $\mu\text{m}$  to 0.9  $\mu\text{m}$  (Figs. 1e–h; 2a,b,e,f; 3 and 4a,b,e,f). Fossilised pigment epithelium and its fibrous structures (Fig. 2c,d) are also preserved in the distal part of the cone and rod cells; these are comparable to those of the pigment epithelium of the extant house sparrow (Figs. 2g,h and 4g). The fossil cones, rods, and oil droplets are preserved rather flattened (Fig. 2a–d), and look like those of the natural dried extant house sparrow (Fig. 4e–h).

The house sparrow and the extant Japanese quail identifies a common tendency between the frequency distribution of area of oil droplets and their associated cone photoreceptors (cone types in Figs. 6 and 7; Tables 1 and 2); specifically, the ultraviolet (UVS) and short-wavelength sensitive cones (SWS) are smallest (Figs. 6b, c and 7b, c), the medium-wavelength sensitive cones (MWS) are mid-sized (Figs. 6d and 7d), and the long-wavelength sensitive cones (LWS) are the largest (Figs. 6f and 7f). In both samples from the extant birds, the frequency distribution of the area of the individual oil droplets also correlates with overall cone type (Figs. 6a–f and 7a–f). Further analysis was performed on the extant house sparrow, as it has a similar size range of oil droplets to the fossil bird. The result of a Mann-Whitney *U* test (Mann and Whitney, 1947) showed that each oil-droplet colour can be distinguished statistically ( $p < 0.05$ ,  $1 - \beta > 0.8$ ), except for the combination of the dark green/red oil droplets (Table 3). The result suggests that four morphological types of oil droplets occur in the extant house sparrow.

To determine the size (maximum projected area) differences among the fossilised oil droplets, and to assess whether the oil droplet size is comparable with that of the extant house sparrow, we examined the frequency distribution of the maximum projected area of fossil oil droplets and the size range of the oil droplets of the extant house sparrow (Fig. 8). The fossil oil droplets exhibited a broad range of sizes, correlating with the UVS to LWS (Table 4).

**Table 2.** Area of oil droplets in an extant Japanese quail *Coturnix japonica*. The cone type to which each oil droplet belongs was determined based on the methods of Kolb and Jones (1982).

No.	Cone type	Area of oil droplet ( $\mu\text{m}^2$ )	No.	Cone type	Area of oil droplet ( $\mu\text{m}^2$ )
1	red	5.5	255	violet	0.7
2	violet	1.1	256	red	3.8
3	red	4.5	257	violet	0.5
4	red	3.8	258	violet	0.8
5	red	5.9	259	red	3.1
6	red	4.0	260	violet	0.5
7	green	3.2	261	green	1.7
8	red	5.7	262	double	1.7
9	green	2.4	263	double	2.6
10	green	3.0	264	double	1.7
11	violet	1.0	265	green	1.8
12	green	1.9	266	violet	0.6
13	red	4.9	267	green	1.8
14	blue	1.5	268	green	1.4
15	red	4.6	269	red	3.3
16	green	1.8	270	green	1.0
17	violet	1.0	271	green	1.6
18	red	5.6	272	red	4.6
19	red	4.2	273	green	1.6
20	red	6.2	274	green	1.2
21	red	4.3	275	red	4.6
22	red	4.8	276	green	1.7
23	green	1.9	277	green	1.0
24	green	2.2	278	green	1.1
25	red	4.7	279	blue	0.9
26	red	4.3	280	green	1.1
27	violet	1.1	281	green	1.7
28	blue	1.0	282	green	1.6
29	blue	0.9	283	red	4.1
30	double	3.0	284	green	1.4
31	violet	0.6	285	violet	0.6
32	red	5.1	286	violet	0.4
33	green	2.0	287	red	3.6
34	blue	1.1	288	green	1.5
35	red	4.6	289	violet	0.7
36	green	3.8	290	green	2.4
37	violet	0.9	291	violet	0.7

(Continued)

**Table 2.** (Continued)

No.	Cone type	Area of oil droplet ( $\mu\text{m}^2$ )	No.	Cone type	Area of oil droplet ( $\mu\text{m}^2$ )
38	green	2.3	292	green	1.2
39	violet	1.1	293	green	2.1
40	blue	0.7	294	green	1.6
41	double	2.8	295	green	1.8
42	red	4.7	296	green	1.1
43	green	1.1	297	green	1.2
44	green	1.2	298	violet	0.4
45	red	4.3	299	blue	0.7
46	blue	0.8	300	green	1.6
47	green	1.3	301	red	3.8
48	green	1.3	302	green	1.6
49	violet	0.7	303	green	1.9
50	violet	1.3	304	green	2.1
51	red	5.0	305	green	2.1
52	green	2.9	306	violet	0.5
53	double	2.8	307	violet	1.1
54	green	1.8	308	green	1.7
55	green	2.2	309	blue	0.4
56	violet	1.2	310	red	5.9
57	red	4.1	311	green	1.7
58	green	1.5	312	green	1.9
59	violet	1.1	313	green	1.8
60	green	1.7	314	green	1.6
61	green	2.1	315	green	2.2
62	red	5.7	316	red	4.4
63	blue	1.2	317	green	1.5
64	red	4.1	318	red	5.4
65	blue	0.8	319	green	1.7
66	green	1.8	320	green	1.4
67	red	4.0	321	green	1.5
68	double	2.6	322	violet	0.5
69	red	4.3	323	green	1.9
70	green	2.6	324	violet	0.4
71	green	2.2	325	red	4.7
72	green	2.2	326	blue	0.5
73	green	2.0	327	red	5.0
74	blue	0.8	328	green	1.8
75	red	3.5	329	red	5.1
76	violet	0.6	330	green	1.5

(Continued)

**Table 2.** (Continued)

No.	Cone type	Area of oil droplet ( $\mu\text{m}^2$ )	No.	Cone type	Area of oil droplet ( $\mu\text{m}^2$ )
77	violet	0.6	331	green	2.7
78	green	1.9	332	green	1.8
79	violet	1.1	333	green	1.7
80	red	3.9	334	green	1.4
81	blue	0.5	335	green	1.5
82	red	4.5	336	red	4.5
83	green	1.9	337	green	1.4
84	green	2.1	338	green	2.2
85	violet	0.8	339	green	2.2
86	red	5.0	340	green	1.5
87	blue	0.7	341	violet	0.8
88	red	3.7	342	green	2.2
89	green	1.7	343	red	5.6
90	green	1.8	344	violet	0.4
91	green	1.5	345	green	2.1
92	violet	0.4	346	blue	0.4
93	red	3.4	347	green	1.7
94	green	2.0	348	green	2.3
95	green	1.6	349	green	1.3
96	blue	1.2	350	violet	0.4
97	green	1.7	351	green	1.6
98	violet	0.6	352	violet	0.6
99	red	4.8	353	violet	0.5
100	green	2.2	354	green	1.5
101	green	1.9	355	green	1.5
102	green	1.4	356	violet	0.4
103	green	2.3	357	green	1.2
104	green	1.7	358	red	4.7
105	red	4.8	359	green	1.7
106	green	1.4	360	green	1.5
107	green	2.0	361	red	5.2
108	double	1.5	362	green	2.3
109	green	1.9	363	double	1.7
110	red	4.8	364	double	1.7
111	red	4.5	365	red	4.7
112	violet	0.8	366	green	1.2
113	green	1.6	367	green	1.8
114	green	2.3	368	green	1.8
115	violet	0.9	369	green	1.6

(Continued)

**Table 2.** (Continued)

No.	Cone type	Area of oil droplet ( $\mu\text{m}^2$ )	No.	Cone type	Area of oil droplet ( $\mu\text{m}^2$ )
116	red	3.9	370	green	1.5
117	blue	0.9	371	blue	0.5
118	green	1.9	372	green	1.8
119	red	3.9	373	double	2.1
120	red	4.3	374	green	1.7
121	green	1.7	375	violet	0.5
122	green	1.4	376	red	3.9
123	violet	0.4	377	violet	0.8
124	green	1.9	378	green	1.2
125	green	1.6	379	green	1.7
126	violet	0.4	380	blue	0.5
127	red	4.7	381	green	1.7
128	double	2.7	382	violet	0.5
129	green	1.3	383	double	1.4
130	blue	0.6	384	red	5.2
131	green	1.5	385	green	1.9
132	blue	1.0	386	green	1.1
133	red	4.1	387	red	4.8
134	blue	0.9	388	green	1.4
135	green	1.7	389	green	2.2
136	violet	0.8	390	red	4.6
137	green	2.2	391	blue	0.5
138	red	5.3	392	green	1.8
139	blue	0.9	393	green	2.8
140	green	2.3	394	violet	0.4
141	red	4.9	395	green	1.9
142	blue	0.7	396	violet	0.7
143	green	1.8	397	green	2.7
144	green	1.8	398	red	5.1
145	violet	0.7	399	violet	0.5
146	green	1.8	400	green	2.0
147	violet	0.6	401	green	1.7
148	blue	0.3	402	violet	0.4
149	violet	0.6	403	green	2.4
150	green	1.8	404	double	2.3
151	red	5.6	405	double	2.5
152	green	1.5	406	green	2.3
153	violet	0.7	407	violet	0.6
154	green	2.0	408	blue	0.7

(Continued)

**Table 2.** (Continued)

No.	Cone type	Area of oil droplet ( $\mu\text{m}^2$ )	No.	Cone type	Area of oil droplet ( $\mu\text{m}^2$ )
155	violet	0.4	409	green	2.3
156	violet	0.7	410	green	2.1
157	green	1.8	411	red	4.9
158	double	1.6	412	violet	0.4
159	red	4.0	413	blue	0.8
160	green	2.1	414	green	2.3
161	violet	0.5	415	blue	0.5
162	red	3.9	416	blue	0.5
163	blue	0.6	417	green	2.1
164	green	2.1	418	green	2.8
165	violet	0.5	419	red	5.4
166	violet	0.7	420	red	5.0
167	green	1.9	421	red	5.3
168	red	4.8	422	green	2.1
169	violet	0.6	423	violet	0.5
170	double	2.1	424	green	2.3
171	green	1.4	425	red	5.6
172	green	1.8	426	double	2.6
173	violet	0.6	427	violet	0.4
174	green	1.6	428	blue	0.6
175	red	3.9	429	green	2.7
176	green	2.3	430	green	2.4
177	violet	0.7	431	green	2.3
178	violet	0.8	432	green	1.8
179	green	1.5	433	red	3.9
180	red	3.9	434	violet	0.4
181	green	1.7	435	double	2.7
182	green	1.9	436	violet	0.3
183	red	5.8	437	green	1.6
184	green	1.6	438	red	4.0
185	green	1.7	439	red	4.4
186	green	1.4	440	red	4.8
187	red	3.6	441	violet	0.4
188	red	4.4	442	violet	0.4
189	green	1.6	443	double	2.8
190	red	3.9	444	green	1.8
191	blue	0.5	445	green	2.1
192	red	3.9	446	green	2.4
193	blue	1.1	447	red	4.3

(Continued)

**Table 2.** (Continued)

No.	Cone type	Area of oil droplet ( $\mu\text{m}^2$ )	No.	Cone type	Area of oil droplet ( $\mu\text{m}^2$ )
194	double	2.1	448	green	1.7
195	red	3.9	449	green	2.0
196	blue	0.6	450	green	1.7
197	green	1.9	451	violet	0.5
198	red	3.7	452	red	4.6
199	green	1.6	453	green	1.8
200	double	1.8	454	green	2.3
201	double	2.8	455	blue	0.4
202	red	3.9	456	green	2.2
203	green	1.4	457	red	5.5
204	blue	0.9	458	green	2.0
205	green	1.9	459	green	2.1
206	green	2.1	460	red	4.6
207	green	1.6	461	green	1.8
208	red	3.8	462	green	2.1
209	red	4.1	463	green	3.3
210	green	1.6	464	blue	0.6
211	blue	0.6	465	violet	0.5
212	blue	0.5	466	green	2.1
213	green	1.4	467	violet	0.6
214	green	1.3	468	red	5.3
215	green	1.7	469	double	2.2
216	red	3.4	470	blue	0.6
217	green	1.8	471	green	2.1
218	green	1.8	472	green	2.3
219	red	3.5	473	red	4.5
220	green	1.8	474	green	1.6
221	green	2.0	475	blue	0.5
222	violet	0.5	476	green	2.4
223	green	1.8	477	green	2.2
224	red	3.7	478	green	2.2
225	green	1.8	479	blue	0.4
226	violet	0.4	480	violet	0.6
227	violet	0.5	481	red	5.3
228	green	1.5	482	double	1.9
229	red	4.2	483	red	5.2
230	blue	0.5	484	green	2.0
231	red	3.8	485	violet	0.5
232	red	4.9	486	green	2.0

(Continued)

**Table 2.** (Continued)

No.	Cone type	Area of oil droplet ( $\mu\text{m}^2$ )	No.	Cone type	Area of oil droplet ( $\mu\text{m}^2$ )
233	green	1.4	487	red	5.3
234	green	1.2	488	green	1.5
235	red	4.3	489	violet	0.4
236	green	1.4	490	green	2.6
237	green	1.4	491	double	2.1
238	violet	0.5	492	red	4.6
239	blue	0.5	493	green	1.5
240	red	4.5	494	green	2.1
241	green	1.5	495	green	2.5
242	red	4.8	496	red	5.1
243	blue	0.4	497	violet	0.5
244	red	4.4	498	green	1.7
245	blue	0.8	499	green	2.4
246	violet	0.6	500	red	4.8
247	blue	0.5	501	green	1.7
248	violet	0.8	502	blue	0.7
249	violet	0.6	503	violet	0.4
250	red	3.4	504	green	3.2
251	violet	1.0	505	blue	0.5
252	double	2.1	506	red	5.1
253	red	4.5	507	green	2.0
254	green	1.3	508	red	5.2

**Table 3.** Result of a Mann-Whitney *U* test of oil droplets of an extant house sparrow *Passer domesticus*. (a) z score, (b) *p*-value two-tailed, (c) Statistical power ( $1 - \beta$ ).

<b>a</b>	clear	light blue	yellow	dark green	red
clear					
light blue	3.771				
yellow	9.378	7.865			
dark green	9.947	8.096	0.679	<i>z</i>	
red	8.863	7.563	7.079	0.967	
<b>b</b>	clear	light blue	yellow	dark green	red
clear					
light blue	0				
yellow	0	0			

(Continued)

**Table 3.** (Continued)

<b>b</b>	<b>clear</b>	<b>light blue</b>	<b>yellow</b>	<b>dark green</b>	<b>red</b>
dark green	0	0	0.497	<i>p</i>	
red	0	0	0	0.334	
<b>c</b>	<b>clear</b>	<b>light blue</b>	<b>yellow</b>	<b>dark green</b>	<b>red</b>
clear					
light blue	0.999				
yellow	1.000	1.000			
dark green	1.000	1.000	0.252	<i>1-β</i>	
red	1.000	1.000	1.000	1.000	

In order to select the relative quality of statistical models for a given set of data (Tables 1, 2 and 4), the Akaike information criterion (AIC) analysis (Akaike, 1974) was carried out (Table 5). The AIC models suggest that the size range of the fossil oil droplets forms one peak (*directional asymmetry*), the same as those of the extant house sparrow and Japanese quail (Table 5).

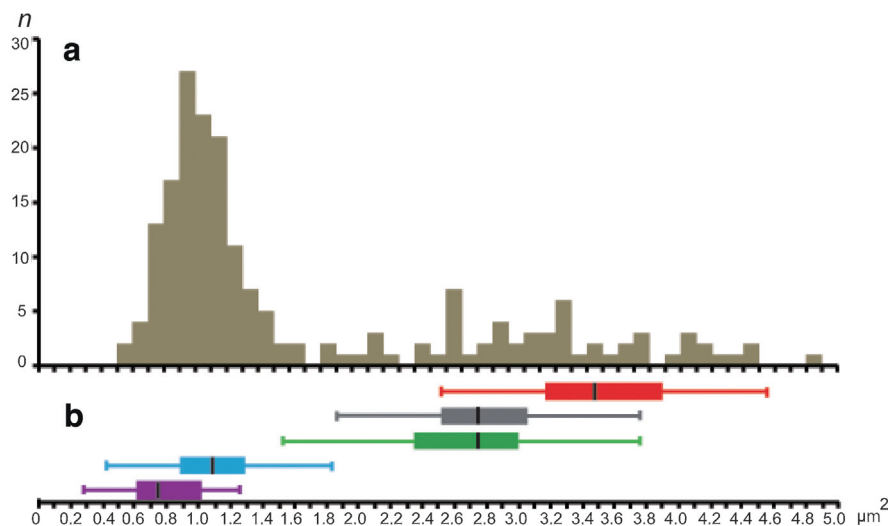


**Fig. 8.** Frequency distribution of the maximum projected area of oil droplets of an Early Cretaceous enantiornithine bird and the range of each oil droplet size in an extant house sparrow. (a) Histogram of fossil oil droplet size based on Table 1. (b) Box-and-whisker diagrams of extant oil droplets size of house sparrow drawn from Fig. 6 and Table 2. The violet, light blue, green, gray, and red ranges correlate with ultraviolet sensitive single cones [UVS], short-wavelength sensitive single cones [SWS], medium-wavelength sensitive single cones [MWS], intermediate sensitive double cones [IWS], and long-wavelength sensitive single cones [LWS], respectively.

**Table 4.** Area of oil droplets in an Early Cretaceous enantiornithine bird.

No.	Cone type	Area of oil droplet ( $\mu\text{m}^2$ )	No.	Cone type	Area of oil droplet ( $\mu\text{m}^2$ )
1	-	1.1	98	-	0.7
2	-	0.6	99	-	3.2
3	-	0.9	100	-	1.4
4	-	0.8	101	-	3.4
5	-	1.2	102	-	1.0
6	-	3.7	103	-	1.1
7	-	0.8	104	-	1.1
8	-	0.8	105	-	1.0
9	-	2.4	106	-	1.0
10	-	0.8	107	-	3.2
11	-	2.8	108	-	2.6
12	-	0.6	109	-	1.0
13	-	0.7	110	-	1.0
14	-	2.6	111	-	0.7
15	-	2.6	112	-	0.9
16	-	0.9	113	-	0.9
17	-	0.9	114	-	0.7
18	-	1.2	115	-	0.9
19	-	0.7	116	-	1.1
20	-	3.0	117	-	0.8
21	-	3.2	118	-	2.5
22	-	0.7	119	-	3.2
23	-	0.6	120	-	3.0
24	-	0.7	121	-	1.0
25	-	2.1	122	-	0.9
26	-	0.5	123	-	0.9
27	-	1.0	124	-	0.8
28	-	0.5	125	-	1.2
29	-	0.6	126	-	1.2
30	-	3.6	127	-	1.0
31	-	1.0	128	-	3.2
32	-	3.6	129	-	1.0
33	-	0.7	130	-	1.1
34	-	3.7	131	-	1.3
35	-	1.3	132	-	1.2
36	-	0.8	133	-	0.9
37	-	1.1	134	-	1.8

*(Continued)*

**Table 4.** (Continued)

No.	Cone type	Area of oil droplet ( $\mu\text{m}^2$ )	No.	Cone type	Area of oil droplet ( $\mu\text{m}^2$ )
38	-	0.8	135	-	0.8
39	-	1.1	136	-	1.1
40	-	3.7	137	-	2.7
41	-	0.7	138	-	1.9
42	-	0.8	139	-	4.1
43	-	3.1	140	-	1.5
44	-	4.0	141	-	0.8
45	-	1.0	142	-	0.8
46	-	0.5	143	-	0.9
47	-	1.0	144	-	1.0
48	-	0.9	145	-	1.1
49	-	1.2	146	-	2.5
50	-	2.8	147	-	0.9
51	-	2.8	148	-	0.9
52	-	3.9	149	-	1.3
53	-	1.7	150	-	4.4
54	-	1.0	151	-	2.0
55	-	1.1	152	-	0.8
56	-	0.9	153	-	1.9
57	-	0.9	154	-	2.9
58	-	0.8	155	-	3.2
59	-	1.6	156	-	1.0
60	-	1.4	157	-	0.9
61	-	1.1	158	-	4.5
62	-	4.2	159	-	1.2
63	-	1.3	160	-	1.2
64	-	4.0	161	-	4.2
65	-	0.9	162	-	4.3
66	-	1.0	163	-	0.7
67	-	0.9	164	-	3.2
68	-	1.1	165	-	3.2
69	-	0.9	166	-	1.3
70	-	0.9	167	-	1.1
71	-	0.9	168	-	0.9
72	-	0.9	169	-	2.9
73	-	0.9	170	-	0.9
74	-	0.7	171	-	1.0
75	-	0.5	172	-	1.1

(Continued)

**Table 4.** (Continued)

No.	Cone type	Area of oil droplet ( $\mu\text{m}^2$ )	No.	Cone type	Area of oil droplet ( $\mu\text{m}^2$ )
76	-	0.7	173	-	1.1
77	-	0.7	174	-	2.8
78	-	0.7	175	-	0.9
79	-	3.1	176	-	0.9
80	-	4.2	177	-	1.0
81	-	0.7	178	-	0.9
82	-	0.9	179	-	1.0
83	-	0.9	180	-	0.8
84	-	1.3	181	-	0.9
85	-	0.5	182	-	2.4
86	-	3.2	183	-	0.9
87	-	0.9	184	-	2.5
88	-	3.4	185	-	1.0
89	-	4.9	186	-	2.3
90	-	3.7	187	-	0.6
91	-	2.1	188	-	2.5
92	-	0.6	189	-	1.0
93	-	0.8	190	-	2.9
94	-	0.7	191	-	1.1
95	-	3.3	192	-	1.0
96	-	1.3	193	-	2.1
97	-	1.0			

**Table 5.** Basic statistics and AIC values for the FA, DA, AS, and Skewed AS models to discriminate the type of asymmetry for an enantiornithine fossil bird, house sparrow and Japanese quail. n = number of specimens, SD = standard deviation, FA = fluctuating asymmetry, DA = directional asymmetry, AS = Antisymmetry.

Specimens	n	Mean	SD	AIC for each model			
				FA	DA	AS	Skewed AS
Enantiornithes fossil bird	193	1.59	1.10	804.43	<b>586.50</b>	806.35	588.50
House sparrow ( <i>Passer domesticus</i> )	316	2.37	1	1498.4	<b>923.17</b>	1354.08	925.17
Japanese quail ( <i>Coturnix japonica</i> )	508	2.16	1.5	2422.4	<b>1841.19</b>	2420.84	1843.19

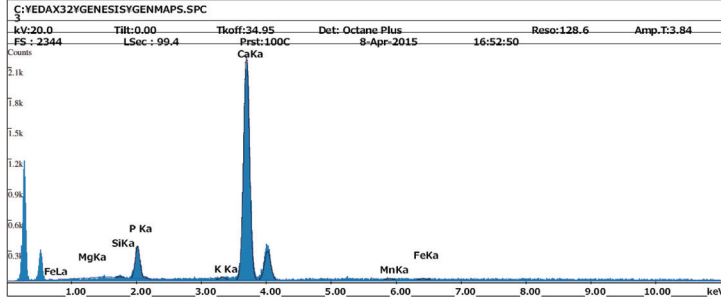
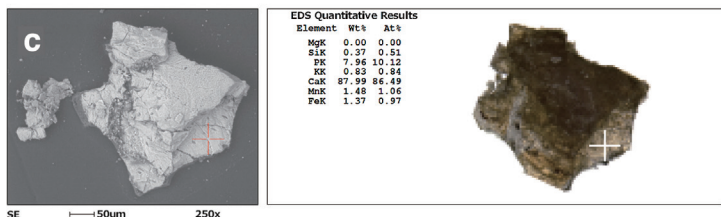
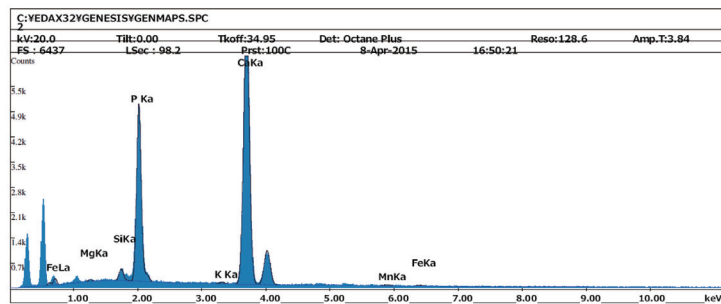
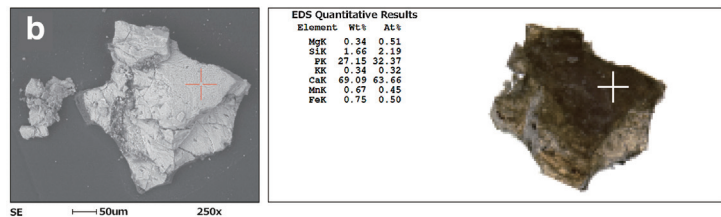
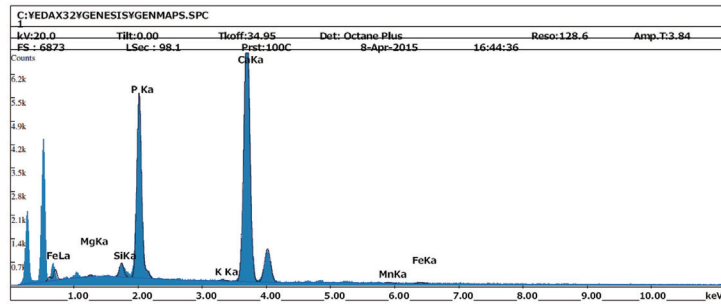
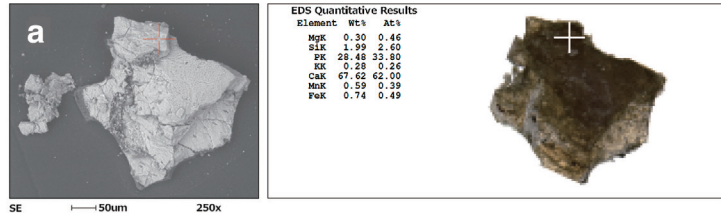
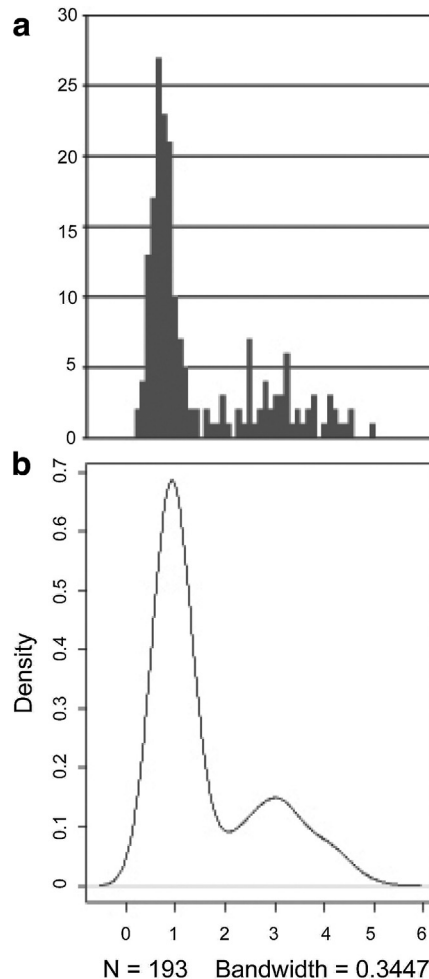


**Fig. 9.** Elemental spectral patterns of three points of a fragment of fossil retina of an Early Cretaceous enantiornithine bird and the distribution of elements. (a,b) Spectral patterns from retinal region (black coloured area). (c) Spectral patterns from bone region (light-yellow coloured area).

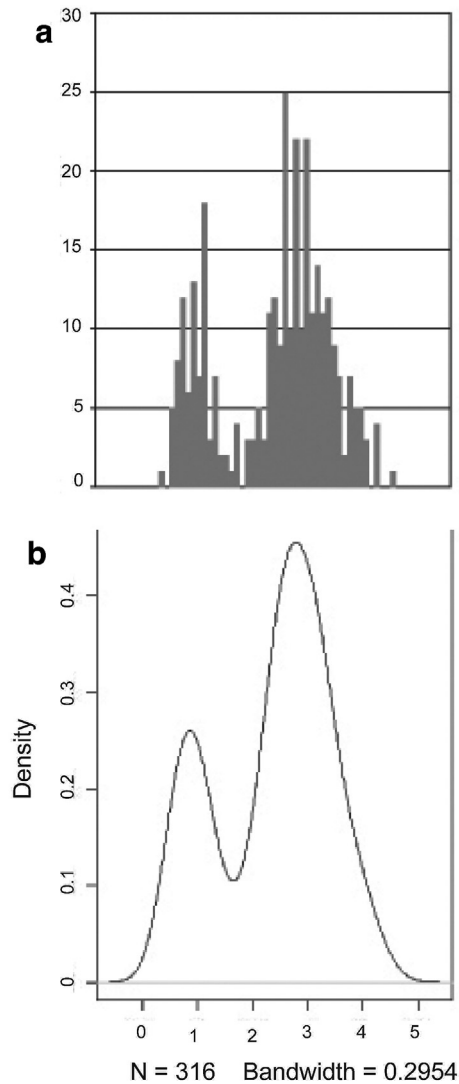
Elemental distribution and spectral patterns of the fossil bird sample showed that calcium and phosphate dominated both the retinal and bone areas (Fig. 5), but a higher concentration of phosphate was detected in the retinal area than in the bone area (Fig. 9).



**c**

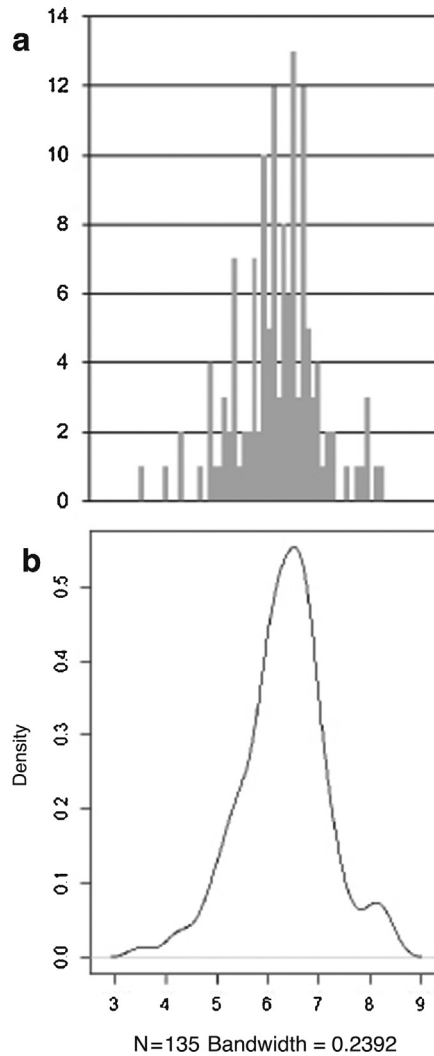
Avian (Fossil)					
	$k = 1$	$k = 2$	$k = 3$	$k = 4$	$k = 5$
<b>P value</b>	0	0.81782	0.58659	0.34735	0.07207

**Fig. 10.** Frequency distribution of the cross-sectional area of oil droplets of a Cretaceous enantiornithine bird. (a) Histogram of oil droplet size. (b) Kernel density estimation of (a). (c) Result of number of modes ( $k$ ) and  $p$ -values.



Avian (House sparrow)					
	$k = 1$	$k = 2$	$k = 3$	$k = 4$	$k = 5$
<b>P value</b>	0	0.72773	0.79880	0.80681	0.52252

**Fig. 11.** Frequency distribution of the cross-sectional area of oil droplets of an extant house sparrow *Passer domesticus*. (a) Histogram of oil droplet size. (b) Kernel density estimation of (a). (c) Result of number of modes ( $k$ ) and  $p$ -values.



Avian (Ural owl)					
	$k = 1$	$k = 2$	$k = 3$	$k = 4$	$k = 5$
<i>P</i> value	0.38223	0.24124	0.29530	0.43443	0.53754

**Fig. 12.** Frequency distribution of the cross-sectional area of oil droplets of an extant Ural owl *Strix uralensis*. (a) Histogram of oil droplet size. (b) Kernel density estimation of (a). (c) Result of number of modes ( $k$ ) and  $p$ -values.

**Table 6.** Area of oil droplets in an extant Ural owl *Strix uralensis*. The area of each oil droplet and its cone type were determined based on the literature given in Gondo and Ando (1995).

No.	Cone type	Area of oil droplet ( $\mu\text{m}^2$ )	No.	Cone type	Area of oil droplet ( $\mu\text{m}^2$ )
1	pale green	5.2	69	pale green	6.8
2	"	6.0	70	"	5.5
3	"	5.4	71	"	6.5
4	"	5.6	72	"	5.6
5	"	6.3	73	"	7.7
6	"	5.8	74	"	6.3
7	"	6.2	75	"	5.9
8	"	7.0	76	"	7.3
9	"	5.8	77	"	6.9
10	"	6.5	78	"	5.2
11	"	4.1	79	"	7.1
12	"	4.9	80	"	6.8
13	"	5.8	81	"	6.6
14	"	5.2	82	"	6.8
15	"	6.9	83	"	5.3
16	"	6.3	84	"	4.4
17	"	6.0	85	"	4.9
18	"	7.2	86	"	6.8
19	"	8.2	87	"	6.8
20	"	6.2	88	"	6.8
21	"	7.3	89	"	3.5
22	"	6.3	90	"	8.1
23	"	6.7	91	"	6.2
24	"	6.2	92	"	5.0
25	"	7.5	93	"	6.4
26	"	6.0	94	"	6.3
27	"	5.8	95	"	6.1
28	"	5.7	96	"	5.8
29	"	6.7	97	"	6.3
30	"	6.4	98	"	6.5
31	"	5.5	99	"	6.7
32	"	5.9	100	"	6.5
33	"	5.2	101	"	8.0
34	"	4.7	102	"	6.8
35	"	6.6	103	"	7.1

(Continued)

**Table 6.** (Continued)

No.	Cone type	Area of oil droplet ( $\mu\text{m}^2$ )	No.	Cone type	Area of oil droplet ( $\mu\text{m}^2$ )
36	"	7.5	104	"	6.9
37	"	4.9	105	"	6.3
38	"	6.7	106	"	6.7
39	"	5.4	107	"	6.0
40	"	6.0	108	"	5.5
41	"	5.4	109	"	5.5
42	"	6.1	110	"	8.3
43	"	6.3	111	"	8.4
44	"	5.8	112	"	6.8
45	"	6.0	113	"	6.4
46	"	6.7	114	"	7.1
47	"	6.7	115	"	6.1
48	"	5.0	116	"	6.6
49	"	6.1	117	"	6.7
50	"	7.2	118	"	7.0
51	"	7.0	119	"	6.1
52	"	6.6	120	"	6.3
53	"	6.7	121	"	6.6
54	"	6.3	122	"	6.5
55	"	7.4	123	"	6.4
56	"	7.9	124	"	5.4
57	"	6.4	125	"	6.0
58	"	6.0	126	"	6.1
59	"	6.7	127	"	5.8
60	"	6.3	128	"	6.7
61	"	6.9	129	"	6.5
62	"	6.5	130	"	6.5
63	"	8.2	131	"	6.8
64	"	7.2	132	"	6.1
65	"	6.0	133	"	5.4
66	"	6.5	134	"	4.3
67	"	6.8	135	"	7.2
68	"	6.1			

#### 4. Discussion and conclusion

This paper reports a unique case of a preserved retina in a fossil bird, including the only record of avian fossil oil droplets, cones and rods, and pigment epithelium. Furthermore, the fossil cones, rods, and oil droplets were rather flattened (Fig. 2a–d) like those of the natural dried extant house sparrow (Fig. 4e–h). This result suggests that the fossil retina was dried (thereby indicating that the bird had already died) before it was transported into water to become preserved as a fossil. Elemental spectral patterns denoted a higher concentration of phosphate in the retinal area than in the bone area (Fig. 9), indicating that soft tissues were replaced by calcium phosphate under high phosphorus levels in early diagenesis (Maeda et al., 2011; Vannier et al., 2016). These findings provide compelling evidence that the general retinal anatomy of birds was in place 120 Ma. Additionally, the presence of oil droplets of a wide range of sizes indicates that the Cretaceous bird likely possessed colour vision. Further, in terms of the bias towards the smaller end of the potential size distribution, the fossil eye oil droplets are more similar to those of the extant house sparrow than to the extant lizards (Bowmaker et al., 2005).

To extract the size (maximum projected area) differences among fossilised oil droplets, and to determine whether the oil droplet size histogram shows a single peak or not, Silverman's test (Schwaiger and Holzmann, 2013) was carried out (Fig. 10, Table 4). The result showed that the  $p$  value was  $<0.05$  in  $k = 1$ , indicating that there were more than two types of oil droplets based on size (Fig. 10). Our examination of the extant house sparrow also indicates that there are at least two types of oil droplets based on size (Fig. 11,  $p < 0.05$  in  $k = 1$ ). Furthermore, there is a good correlation between the size of an oil droplet and its peak wavelength sensitivity (cone type in Fig. 6); specifically, the ultraviolet (UVS) and short-wavelength sensitive cones (SWS) tend to be distributed in the small size region of the histogram (Figs. 6a–c and 11). However, in a nocturnal bird, the Ural owl *Strix uralensis*, only pale green-coloured oil droplets have been found (Gondo and Ando, 1995). The result of a Silverman's test using Fig. 7 of Gondo and Ando (1995), further suggests a single peak (Fig. 12, Table 6,  $p > 0.05$  in  $k = 1-5$ ). Therefore, the histogram of the fossil bird and extant house sparrow shows two peaks based on Silverman's test and can be discriminated from the nocturnal bird (Ural owl).

As inferred from the opsin genes of extant species, tetrachromatic vision first evolved in jawless fish (Bowmaker, 2008). In reptiles and birds, the performance of cone cells is further enhanced by the addition of oil droplets which transmit specific wavelengths only (Stavenga and Wilts, 2014; Loew et al., 2002). Thus, the discovery of oil droplets in the fossil bird specimen here indicates that the complex optical system of cone cells had already been achieved at least by 120 Ma.

On the other hand, single-coloured oil droplets are found in the snowy owl and king penguin (Gondo and Ando, 1995). The snowy owl and king penguin inhabit snow-covered terrain, or water with a high content of blue light, and so the discrimination of multiple colours is not a selection pressure. A single oil droplet type, or filter, is as efficient at detecting objects against such a background as are multiple colour filters.

To conclude, from an examination of its retina, the Cretaceous enantiornithine bird studied here was probably a diurnal species and possessed colour vision. The frequency distribution analysis of oil droplets in the fossil bird eye appears a useful method to aid the reconstruction of its palaeoecology.

## Declarations

### Author contribution statement

Gengo Tanaka: Conceived and designed the experiments; Performed the experiments; Analyzed and interpreted the data; Contributed reagents, materials, analysis tools or data; Wrote the paper.

Baochun Zhou: Performed the experiments; Analyzed and interpreted the data; Contributed reagents, materials, analysis tools or data; Wrote the paper.

Yunfei Zhang: Contributed reagents, materials, analysis tools or data; Wrote the paper.

David J. Siveter: Analyzed and interpreted the data; Wrote the paper.

Andrew R. Parker: Conceived and designed the experiments; Analyzed and interpreted the data; Wrote the paper.

### Competing interest statement

The authors declare no conflict of interest.

### Funding statement

This work is supported by the MEXT KAKENHI (Grant no. 16K05592 to Gengo Tanaka); it is also partly supported by the Shanghai Municipal Natural Science Foundation (Grant no. 14ZR1427600 to Baochun Zhou).

### Additional information

No additional information is available for this paper.

## Acknowledgments

Yasuhisa Henmi and Motohiro Shimanaga (Kumamoto University) kindly provided experimental facilities. B. Z. and Y. Z. thank Xiaoming Wang (Shanghai Science and Technology Museum) for continuous support. Zhonghe Zhou (Institute of Vertebrate Paleontology and Paleoanthropology, Chinese Academy of Science), Yuguang Zhang (Beijing Museum of Natural History) and Dongyu Hu (Shenyang Normal University) helpfully commented on the identification of the fossil bird specimen.

## References

- Akaike, H., 1974. A new look at the statistical model identification. *IEEE Trans. Automatic Control* 19, 716–723.
- Barden, H.E., Wogelius, R.A., Li, D., Manning, P.L., Edwards, N.P., Van Dongen, B.E., 2011. Morphological and geochemical evidence of eumelanin preservation in the feathers of the Early Cretaceous bird, *Gansus yumenensis*. *PLoS One* 6, e25494.
- Bowmaker, J.K., Loew, E.R., Ott, M., 2005. The cone photoreceptors and visual pigments of chameleons. *J. Comp. Physiol. A* 191, 925.
- Bowmaker, J.K., 2008. Evolution of vertebrate visual pigments. *Vis. Res.* 48, 2022–2041.
- Cheung, D.W.S., Wai, M.S.M., Yew, D.T., 2013. The diversity of cones in the retina of vertebrates: a review. *OA Anat.* 1, 1–6.
- Chiappe, L.M., Walker, C.A., 2002. Skeletal morphology and systematics of the Cretaceous Euenantiornithes (Ornithothoraces: Enantiornithes). In: Chiappe, L.M., Lawrence, M. (Eds.), *Mesozoic Birds: Above the Heads of Dinosaurs*. University of California Press, pp. 240–267.
- Cuthill, I.C., 2006. Color perception. In: Hill, G.E., McGraw, K.J. (Eds.), *Bird Coloration: Mechanisms and Measurements*. Harvard University Press, pp. 3–40.
- Dobson, F.S., 2012. Lifestyles and phylogeny explain bird life histories. *Proc. Natl. Acad. Sci. U. S. A.* 109, 10747–10748.
- Duncan, I.J., Briggs, D.E.G., 1996. Three-dimensionally preserved insects. *Nature* 381, 30–31.
- Faul, F., Erdfelder, E., Lang, A., Buchner, A., 2007. G\*Power 3: a flexible statistical power analysis program for the social, behavioral, and biomedical sciences. *Behav. Res. Methods* 39, 175–191.

- Fröhlich, F., Mayra, A., Riou, B., Secretan, S., 1992. Structures rétiniennes phosphatisées dans l'oeil géant de Dollocaris, un crustacé fossile. *Annals de Paléontologie* 78, 193–204.
- Gondo, M., Ando, H., 1995. Comparative histophysiological study of oil droplets in the avian retina. *Jpn. J. Ornithol.* 44, 81–91.
- Hart, N.S., 2001a. The visual ecology of avian photoreceptors. *Prog. Retinal Eye Res.* 20, 675–703.
- Hart, N.S., 2001b. Variations in cone photoreceptor abundance and the visual ecology of birds. *J. Comp. Physiol. A* 187, 685–698.
- Hart, N.S., 2004. Microspectrophotometry of visual pigments and oil droplets in a marine bird, the wedge-tailed shearwater *Puffinus pacificus*: topographic variations in photoreceptor spectral characteristics. *J. Exp. Biol.* 207, 1229–1240.
- Jiang, B., Harlow, G.E., Wohletz, K., Zhou, Z., Meng, J., 2014. New evidence suggests pyroclastic flows are responsible for the remarkable preservation of the Jehol Biota. *Nat. Commun.* 5, 3151.
- Kolb, H., Jones, J., 1982. Light and electron microscopy of the photoreceptors in the retina of the red-eared slider, *Pseudemys scripta elegans*. *J. Comp. Neurol.* 209, 331–338.
- Kram, Y.A., Mantey, S., Corbo, J.C., 2010. Avian cone photoreceptors tile the retina as five independent, self-organizing mosaics. *PLoS One* 5, e8992.
- Li, Q., Gao, K., Vinther, J., Shawkey, M.D., Clarke, J.A., D'Alba, L., Meng, Q., Briggs, D.E.G., Prum, R.O., 2010. Plumage color patterns of an extinct dinosaur. *Science* 327, 1369–1372.
- Li, Q., Gao, K., Meng, Q., Clarke, J.A., Shawkey, M.D., D'Alba, L., Pei, R., Ellison, M., Norell, M.A., Vinther, J., 2012. Reconstruction of Microraptor and the evolution of iridescent plumage. *Science* 335, 1215–1219.
- Loew, E.R., Fleishman, L.J., Foster, R.G., Provencio, I., 2002. Visual pigments and oil droplets in diurnal lizards: a comparative study of Caribbean anoles. *J. Exp. Biol.* 205, 927–938.
- Maeda, H., Tanaka, G., Shimobayashi, N., Ohno, T., Matsuoka, H., 2011. Cambrian Orsten Lagerstätte from the Alum Shale Formation: fecal pellets as a probable source of phosphorus preservation. *Palaios* 26, 225–231.
- Mann, H.B., Whitney, D.R., 1947. On a test of whether one of two random variables is stochastically larger than the other. *Ann. Math. Stat.* 18, 50–60.

- Ohtsuka, T., 1985. Relation of spectral types to oil droplets in cones of turtle retina. *Science* 229, 874–877.
- Ohtsuka, T., 1989. Retina neural circuit of abstracting color information. *Anim. Physiol.* 6, 49–57 (In Japanese).
- R. Development Core Team, 2013. A language and environment for statistical computing. R Foundation for Statistical Computing, Vienna, Austria. <http://www.R-project.org/>.
- Rasband, W.S., 1997–2012. Image J. U.S. National Institutes of Health, Bethesda Maryland, USA, <http://imagej.nih.gov/ij/>.
- Schoenemann, B., Castellani, C., Clarkson, E.N.K., Haug, J.T., Maas, A., Haug, C., Waloszek, D., 2012. The sophisticated visual system of a tiny Cambrian crustacean: analysis of a stalked fossil compound eye. *Proc. R. Soc. B: Biol. Sci.* 279, 1335–1340.
- Schoenemann, B., Clarkson, E.N.K., 2013. Discovery of some 400 million year-old sensory structures in the compound eyes of trilobites. *Sci. Rep.* 3, 1429.
- Schwaiger, F., Holzmann, H., 2013. Package ‘silvermantest’.
- Stavenga, D.G., Wilts, B.D., 2014. Oil droplets of bird eyes: microlenses acting as spectral filters. *Philos. Trans. R. Soc. B* 369, 20130041.
- Tanaka, G., Parker, A.R., Siveter, D.J., Maeda, H., Furutani, M., 2009. An exceptionally well-preserved Eocene dolichopodid fly eye: function and evolutionary significance. *Proc. R. Soc. B: Biol. Sci.* 279, 1015–1019.
- Tanaka, G., Parker, A.R., Hasegawa, Y., Siveter, D.J., et al., 2014. Mineralized rods and cones suggest colour vision in a 300 Myr-old fossil fish. *Nat. Commun.* 5, 5920.
- Takeyasu, H., 2011. Statistical power analysis with microsoft office excel. *Philologia* 42, 89–105.
- Vannier, J., Schoenemann, B., Gillot, T., Charbonnier, S., Clarkson, E., 2016. Exceptional preservation of eye structure in arthropod visual predators from the Middle Jurassic. *Nat. Commun.* 7, 10320.
- Wilby, D., Toomey, M.B., Olsson, P., Frederiksen, R., Cornwall, M.C., Oulton, R., Kelber, A., Corbo, J.C., Roberts, N.W., 2015. Optics of cone photoreceptors in the chicken (*Gallus gallus domesticus*). *J. R. Soc. Interface* 12, 20150591.
- Xu, X., Zhou, Z., Dudley, R., Mackem, S., Chuong, C.-M., Erickson, G.M., Varricchio, D.J., 2014. An integrative approach to understanding bird origins. *Science* 346, 1253293.

Zhang, F., Kearns, S.L., Orr, P.J., Benton, M.J., Zhou, Z., Johnson, D., Xu, X., Wang, X., 2010. Fossilized melanosomes and the colour of Cretaceous dinosaurs and birds. *Nature* 463, 1075–1078.

Zhou, Z., Barrett, P.M., Hilton, J., 2003. An exceptionally preserved Lower Cretaceous ecosystem. *Nature* 421, 807–814.